Proceedings of the Estonian Academy of Sciences,
2019, **68**, 1, 13–21
https://doi.org/10.3176/proc.2019.1.07
Available online at www.eap.ee/proceedings

MATERIALS SCIENCE

Effects of polypropylene carbonate coating on the degradation and biocompatibility of degradable magnesium alloy AZ31

Zhiwei Zhao[a], Lirong Zhao[b], Xudong Shi[c], Jianfeng Liu[a,d], Yijun Wang[a], Wu Xu[c], Hai Sun[c], Zhuo Fu[a], Bin Liu[a,d*], and Shucheng Hua[e*]

[a] Department of Hand and Foot Surgery, The First Hospital of Jilin University, Changchun, 130021, China
[b] Department of Electrical Diagnosis, The First Hospital of Jilin University, Changchun, 130021, China
[c] Key Laboratory of Polymer Ecomaterials, Changchun Institute of Applied Chemistry, Chinese Academy of Sciences, Changchun, 130022, China
[d] Jilin Province Key Laboratory on Tissue Repair, Reconstruction and Regeneration, Changchun, 130021, China
[e] Department of Respiratory Medicine, The First Hospital of Jilin University, Changchun, 130021, China

Received 15 November 2018, accepted 7 December 2018, available online 21 December 2018

Abstract. The use of magnesium alloys as degradable orthopaedic implants is limited by their rapid degradation in vivo and consequent loss of mechanical integrity before sufficient bone healing has occurred. To address this limitation, we coated the surface of AZ31 magnesium alloys with polypropylene carbonate (PPC). The obtained PPC-coated AZ31 showed reduced surface roughness, hardness, and hydrophilicity compared with bare AZ31. The PPC coating also significantly slowed the degradation of AZ31 in a simulated body fluid. The adherence and proliferation of MC3T3 osteoblastic cells cultured on PPC-coated AZ31 samples demonstrated good biocompatibility. The results of the present study indicate that application of a PPC coating may extend the functional period of AZ31 magnesium implants in vivo to allow sufficient time for bone healing and for the stimulation of new bone formation.

Key words: magnesium alloy, biodegradability, polymer coating, corrosion, biocompatibility, orthopaedic implant.

1. INTRODUCTION

For serious cases of bone fracture, surgical treatment is often necessary to avoid a final outcome of nonunion or malunion [1,2]. Such surgeries often involve the use of internal fixation implants to fix and stabilize the broken bone tissues to permit proper healing. For many years fixation implants were fabricated from inert metallic materials, such as medical-grade stainless steel and titanium alloys, and these implants continue to play a major role in orthopaedics [3]. Although the currently approved metallic implants offer high mechanical strength and toughness [4], these implants are non-degradable, and thus require a second surgery for removal once the fractured bone has healed. Another limitation of the current metallic implants is the difference between their elastic modulus and that of natural bone tissue. The elastic modulus of metallic implants is remarkably higher than that of cortical bone, resulting in a decrease in the internal stress within the treated bone. However, this internal stress is a natural stimulus of bone growth, and reduced bone growth compromises the stability of the implant, an effect that is termed stress

* Corresponding authors, kjkliubin@126.com, shuchenghua@eyou.com

shielding [5,6]. Furthermore, toxic metallic ions can be released from the metallic implants through the in vivo corrosion process, consequently inducing an inflammatory cascade and tissue loss [7,8].

For these and other reasons, much research has been directed at developing degradable internal fixation implants. Degradable metallic implants are designed to provide sufficient strength to support the broken bones in the early period of fracture healing but to gradually degrade via the corrosion process as the bone heals, eliminating the need for a second surgery for implant removal [9]. Among the studied degradable metallic materials, magnesium alloys offer remarkable mechanical strength to support broken bones [10,11]. However, a major drawback of magnesium alloys is that these alloys corrode rapidly in vivo, with the implants potentially losing mechanical integrity before the bone tissue has healed sufficiently to support the stress [12]. Also, as they corrode, these alloys may produce gas at a rate that is too fast for its absorption by the surrounding tissues. To overcome these limitations, a myriad of methods have been tested to slow the corrosion rate of magnesium implants, such as additional alloying, heat treatment, and surface modification [13].

Among these methods, polymer coating has attracted special interest because it is cost-effective and the implant surface can be further functionalized via conjugation of biomolecules to the polymer coating [14]. Several polymers have been applied as coatings on the surface of magnesium alloys [14–20]; however, there were some drawbacks when using them as implants in vivo. For example, the degradation products of polylactide (PLA), poly(lactic-co-glycolic acid) (PLGA), and polycaprolactone (PCL) may induce an inflammatory response or foreign body reaction in vivo [21,22]. Poly(ether imide) (PEI), a non-degradable polymer coated on magnesium, may be hard to be metabolized in body. Therefore, there is an urgent need to explore new biodegradable polymer coatings with better biocompatibility that can be used to control the degradation rate of magnesium alloys.

Polypropylene carbonate (PPC) is a type of degradable polymer synthesized by copolymerization of carbon dioxide and propylene oxide. It is characterized by low density, high specific strength, and strong cohesion between polymer chains, and is mainly used to form barrier materials, foam materials, and polymer electrolytes [23]. Because the degradation products of PPC are carbon dioxide and water, which are readily metabolized within the human body, PPC materials also offer great biocompatibility and have been assessed for applications in drug delivery, as tissue scaffolds, and for other biomedical applications [24–26]. Recently, Manavitehrani et al. reported that PPC together with a starch composite can be well tolerated in vivo as a foreign material, showing much less inflammation within 1 month after implantation than a biodegradable PLA composite, which induces massive immune cell infusion [27]. Moreover, PPC materials offer good flexibility and low breathability, making this polymer an ideal candidate for surface modification of magnesium alloys.

To explore the potential of PPC as a coating polymer for orthopaedic implants, in the present study we deposited PPC onto the surface of the degradable magnesium alloy AZ31. The surface morphology, hardness, and wettability property of the coated alloy were assessed in relation to those of the bare alloy. Furthermore, we studied the effects of the PPC coating on the degradation rate and biocompatibility of AZ31.

2. MATERIALS AND METHODS

2.1. Preparation of PPC-coated magnesium alloy AZ31

Magnesium alloy discs (10 mm × 10 mm × 1.5 mm) and plates (15 mm × 12 mm × 1.5 mm) were machined from AZ31 magnesium alloy rods and plates (Luoyang Shengte Metal Products Co. Ltd), respectively. After having been ground gradually into 1200 grits, the discs and plates were degreased in acetone via an ultrasonic bath for 10 min and descaled in 180 g/L chromic acid for another 10 min. Then they were rinsed with deionized water, dried with warm air, and stored in acetone for further use.

Polypropylene carbonate (weight-average molecular weight (MW) 250 kDa, polydispersity index (PDI) 3.67) was provided by the Changchun Institute of Applied Chemistry, Chinese Academy of Sciences. It was weighed, transferred to a glass beaker, and dissolved in dichloromethane to a concentration of 3% (w/v). For coating with PPC, the AZ31 magnesium alloy discs or plates were removed from acetone, dried with warm air, and then dipped into the PPC solution. The discs or plates were submerged in the PPC solution for 1 min and then withdrawn at the speed of 1 mm/s. After that, the samples were dried at room temperature for 24 h and in vacuum for 48 h to complete the PPC coating process.

2.2. Assessment of surface morphology, roughness, and coating thickness

The surface morphology of the bare magnesium samples (Bare-Mg) and PPC-coated samples (M-Mg) was assessed by field emission scanning electron

microscopy (FE-SEM, SU8000, Hitachi Ltd). The samples were imaged without gold spraying to avoid artefacts. The acceleration voltage was set at 3 kV, and the working distance was set at 8.4–8.6 mm.

To determine the thickness of the PPC coating on the samples, plates were prepared by dipping only half of the plates into the PPC solution, while the other half of the plates were kept out of the solution. After the coating procedure, a step line between the bare and coated surfaces was obtained at the middle of the sample. The surface roughness and coating thickness perpendicular to the step line were measured by a profilometer (Dektak 150, Veeco Instruments Inc.). The sampling length was 3000 μm with a stylus force set at 1.00 mg. The roughness of the bare and coated surfaces was assessed separately. The thickness of the coating was calculated based on the height difference between the bare and the coated surface. Five sampling lengths were measured for each sample, with three samples assessed for each group.

2.3. Assessment of surface hardness

Because the roughness of magnesium samples would interfere with the measurement of surface hardness, glass plates were chosen as the base materials for surface hardness measurement. Glass plates coated with PPC (M-Glass) were obtained by using the same procedures detailed above. The surface hardness was determined with a Nano Indenter (G200, Agilent) and calculated from the obtained load–displacement curve by using the manufacturer's software. The indentation depth limit was set at 50 nm. The indentation tests were applied at five sampling points for each sample and repeated for three samples in each group.

2.4. Assessment of surface wettability

The water contact angle on the Bare-Mg and M-Mg was determined by a drop shape analyser using the sessile drop method with 2 μL DI H_2O. The assessment was performed at three different locations on each sample and repeated for three samples in each group.

2.5. Fourier transform infrared spectroscopy (FTIR) characterization

To determine the composition of the surface coating, a PPC film was prepared as a control. The surface chemical compositions of the coated and bare magnesium plates and PPC film were characterized by attenuated total reflection (ATR)-FTIR (VERTEX 70, Bruker Corporation). The measured spectroscopy data were imported into Origin 9.0 software and normalized for analysis of the corresponding infrared absorption peaks.

2.6. In vitro degradation experiment

Simulated body fluid (SBF) was prepared as a mixture of 5.403 g/L NaCl, 0.504 g/L $NaHCO_3$, 0.426 g/L Na_2CO_3, 0.225 g/L KCl, 0.230 g/L $K_2HPO_4{\cdot}3H_2O$, 0.311 g/L $MgCl_2{\cdot}6H_2O$, 0.8 g/L NaOH, 17.892 g/L HEPES, 0.293 g/L $CaCl_2$, and 0.072 g/L Na_2SO_4 and adjusted to pH 7.4 with 1.0 M NaOH [28]. The magnesium samples were immersed in a 250 mL glass beaker with SBF (the ratio of SBF volume to sample surface area was set at approximately 122 mL : 1 cm^2). To assess the rate of degradation, a glass funnel and burette were connected, inverted, and placed on the top of a beaker. The volume of the hydrogen gas produced during the degradation was determined by the drop of the level of the liquid in the burette. The volume in the burette was measured every 12 h in the first day and every 24 h in the following days. Because the amount of the degraded magnesium alloy is proportional to that of the produced gas according to the related chemical reaction, the hydrogen evolution could reflect the degradation rate of the corresponding group [29]. The whole system was kept at 10.4–16.0 °C and atmospheric pressure to ensure comparability between samples.

2.7. Cell culture

Both direct and indirect cell culture experiments were performed in this study. MC3T3 cells were cultured in Dulbecco's modified eagle medium (DMEM, Gibco, Thermo Fisher Scientific Inc.) supplemented with 10% fetal bovine serum (Kangyuan, Tianjin) and 1% penicillin–streptomycin solution (Solarbio, Beijing). All cellular experiments were performed once the cells had grown into the logarithmic growth phase.

For the direct cell experiment, 500 μL of MC3T3 cell solution (2×10^4 cells/mL) was added to wells of a 48-well cell culture plate that already contained a bare or PPC-coated magnesium disc. Then the cells were incubated in a humid 5% CO_2 environment at 37 °C with no exchange of the culture medium. The cells on the discs were incubated for 6 h, 1 d, or 3 d before live–dead staining (calcein-AM and propidium iodide (PI), BestBio, Shanghai) according to the manufacturer's protocol and observed under a fluorescent inverted microscope (ECLIPSE Ti-S, Nikon Instruments Inc.) to assess the adhesion and proliferation of cells on the magnesium discs.

For the indirect experiment, 100 μL of MC3T3 cell solution (2×10^4 cells/mL) was added to wells within a

96-well cell culture plate. After 24 h of incubation, the original cell culture medium was discarded and replaced by a mixture of 50 µL of fresh culture medium and 50 µL of SBF or degradation extract from Bare-Mg or degradation extract from M-Mg. The degradation extracts were taken from the previous in vitro degradation experiment after 26 days of degradation of Bare-Mg or M-Mg. The cells were then incubated in a humid 5% CO_2 environment at 37 °C with no exchange of the culture medium. The cells were incubated for 1 day or 3 days and then analysed using the CCK-8 assay (Dojindo, Japan) according to the manufacturer's protocol. The absorbance value reflecting the proliferation of cells was measured in each well by a microplate reader (ELx808, BioTek Instruments Inc.).

2.8. Statistical analysis

The data for the mechanical properties of the tested materials, the in vitro degradation of coated and non-coated magnesium alloys, and cell proliferation on the coated and non-coated magnesium alloys were presented as mean ± standard deviation (SD). Statistical analysis was performed using Student's *t*-test or one-way analysis of variance (ANOVA) with Tukey's post hoc test and a significance level set at 0.05.

3. RESULTS

3.1. Surface morphology and roughness of PPC-coated and non-coated magnesium alloys

Representative scanning electron microscopy (SEM) images of the bare magnesium (Bare-Mg) and PPC-coated magnesium (M-Mg) samples are shown in Fig. 1A and 1B. In these images, tiny parallel scratches can be seen on the Bare-Mg surface after grinding. After coating with PPC, the surface scratches were smoothed, but the direction of the scratches was preserved. Consistent with the differences observed by SEM, the surface roughness of Bare-Mg of approximately 165.1 ± 18.8 nm was reduced to 136.3 ± 23.8 nm after the addition of the PPC coating (Fig. 1C). The thickness of the PPC coating layer was determined to be approximately 250 nm by calculating the height difference between the coated and bare surfaces of the samples.

3.2. Confirmation of PPC coating by FTIR

To further confirm the successful coating of the Mg samples with PPC, the ATR-FTIR spectra of AZ31 magnesium samples were measured before and after PPC deposition (Fig. 2). The spectra for M-Mg samples exhibited several peaks from organic groups, such as the

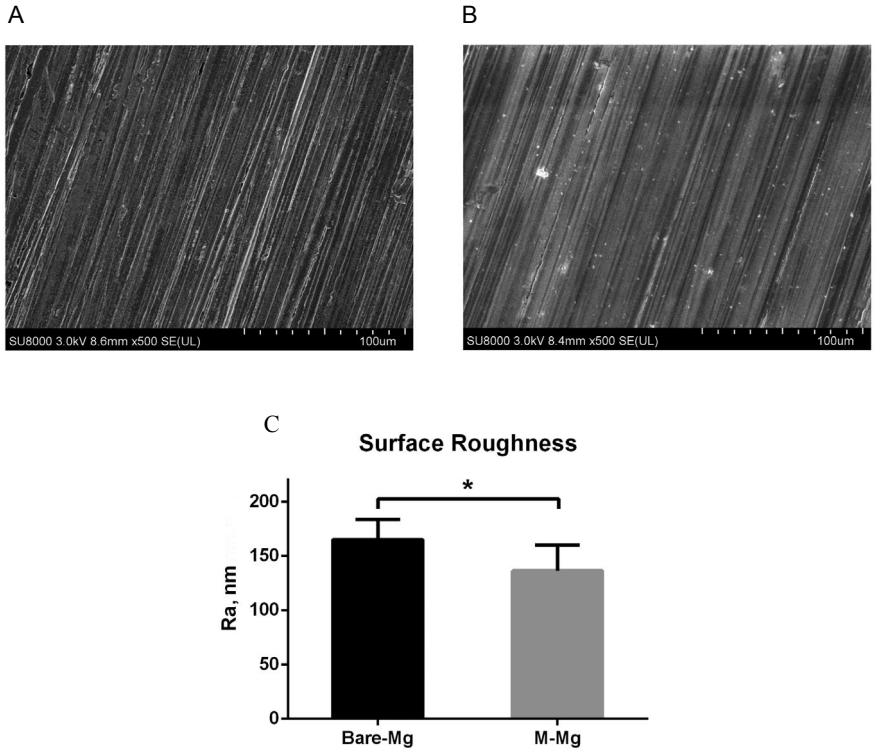

Fig. 1. Representative SEM images of Bare-Mg (A) and M-Mg (B). Surface roughness of Bare-Mg and M-Mg (C). *$p < 0.05$.

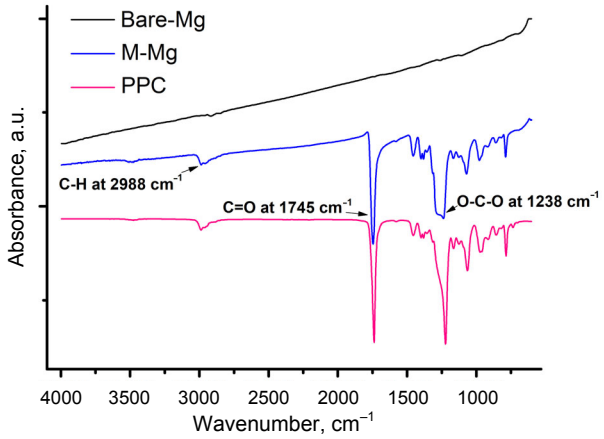

Fig. 2. ATR-FTIR spectra for Bare-Mg (black curve), M-Mg (blue curve), and PPC film (pink curve) surfaces.

absorbance from C–H groups centred at 2988 cm^{-1} and the absorbance from C=O groups centred at 1745 cm^{-1} as well as O–C–O groups centred at 1238 cm^{-1}, which are consistent with the characterized spectra of PPC film in pink colour. In contrast, the spectra of Bare-Mg samples showed no peaks due to the lack of surface organic groups. These results indicate that PPC was successfully deposited onto the surface of the Mg samples.

3.3. Surface wettability and hardness of PPC-coated and non-coated samples

Wettability is an important surface property for implants, which influences the response to the material in vivo [30,31]. To assess the change in wettability with polymer coating, the water contact angles on the surfaces of Mg samples before and after PPC coating were determined by a drop shape analyser by applying the sessile drop method. The water contact angle increased with the addition of the polymer coating, from 57.3 ± 3.5° on the Bare-Mg samples to 77.6 ± 1.2° on the M-Mg samples (Fig. 3), indicating that the surface hydrophilicity decreased a little after polymer deposition. Hao et al. found that the surface of moderate wettability can promote the adhesion, proliferation, and osteogenic differentiation of mesenchymal stem cells and that the most favoured angle slightly differs among experiments and cell origins, roughly lying in the range of 20–90° [32]. Therefore, the small increase in the contact angle after PPC coating may not be unfavourable to the biocompatibility of implants.

The surface hardness is another important property that influences the ability of implants to resist stress. For nanoindentation measurement, the roughness of

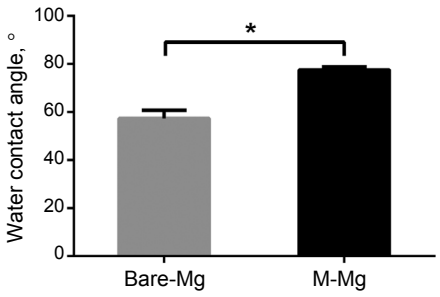

Fig. 3. Water contact angle measurements on Bare-Mg and M-Mg surfaces. *$p < 0.05$.

magnesium samples would strongly interfere with the results, so glass plates were chosen as the base materials to study the influence of PPC coating on the surface hardness. As shown in Fig. 4, the surface hardness of the PPC layer was 0.12 ± 0.06 GPa, which was significantly less than that of the glass substrate (8.38 ± 1.21 GPa). In a specialized research concerning the nanoindentation measurement of magnesium, the surface hardness of AZ31 was found to be in a range of 1.2–1.9 GPa, which is apparently more than that of M-Mg [33]. Although a reduced surface hardness could increase the risk of damage to implants, this disadvantage is common for all types of polymer-coated implants. Moreover, the flexibility of PPC is significantly greater than that of many other polymers such as PLA and PLGA [23], and greater flexibility of coating layers may protect implants from breaking during the deformation and shaping procedure in use. Xu et al. compared SEM images of AZ31 coated with PLA and PCL and found that the PCL coating confers higher flexibility and greater resistance to breakage and corrosion [34]. A similar observation was also reported by Jo et al. from their finite element method (FEM) simulation of magnesium materials [35]. Therefore, the flexibility achieved with PPC coating may allow a magnesium alloy implant to better resist breakage and corrosion during deformation and usage.

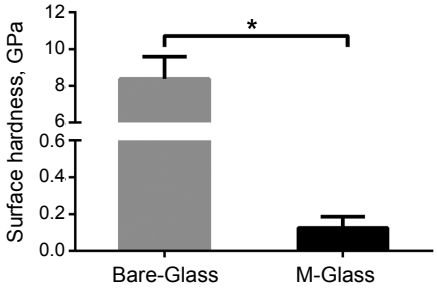

Fig. 4. Surface hardness of bare glass and PPC layer on glass. *$p < 0.05$.

3.4. In vitro degradation behaviour of PPC-coated and non-coated magnesium alloys

The degradation rate of magnesium alloys with or without PPC coating was determined by assessing the volume of the generated hydrogen gas. As shown in Fig. 5, the rate of degradation of Bare-Mg was rapid in the first 200 h (early phase) and thereafter gradually slowed. In contrast, the rate of degradation of M-Mg remained at a low speed in the SBF. The slowed degradation of Bare-Mg after 200 h may be caused by the formation of a corrosion product layer on the surface of the magnesium alloy, which mainly consists of carbonated calcium phosphate [36,37]. Because this layer formed after some time during degradation, the protective effect for Bare-Mg was only observed in the late phase (after 200 h). On the other hand, the PPC layer protected M-Mg samples from rapid degradation in the early phase and slowed the degradation rate by about 50%. These results suggest that M-Mg may corrode slowly in vivo, which would significantly extend the period when the implants can provide sufficient support for fracture fixation.

3.5. Cellular compatibility of PPC-coated and non-coated magnesium alloys

The osteogenic activity on the surface of orthopaedic implants is critical to fracture healing [38–40]. To investigate the effect of the PPC coating on osteoblast cell growth, MC3T3 cells were cultured on the surfaces of the Bare-Mg and M-Mg discs (direct cell culture experiment) or in media containing the degradation extract from Bare-Mg and M-Mg samples (indirect cell culture experiment). Figure 6 shows representative images of live–dead staining of MC3T3 cells on the surface of the Bare-Mg and M-Mg after 6 h, 1 day, and 3 days in culture. The MC3T3 cells adhered to the surface of Bare-Mg after 6 h of incubation but showed little proliferation over the next 3 days. The MC3T3 cells also successfully adhered to the surface of M-Mg during 6 h of incubation, but then showed continued proliferation over the next 3 days in culture. The density of live cells on the M-Mg surface was considerably higher than that on the Bare-Mg surface after 3 days. We speculate that in the first 6 h of incubation, the degradation of magnesium was relatively minimal for both Bare-Mg and M-Mg samples, and thus, MC3T3 cell adherence did not differ much between these two materials. However, with additional time in culture, the concentration of Mg ions released from the Bare-Mg samples increased more rapidly than that from the M-Mg samples due to the faster degradation of the Bare-Mg samples in the cellular culture medium. Because of the small ratio of the culture medium volume to the sample surface area as 0.24 mL : 1 cm^2, the concentration of Mg ions could have reached toxic levels and thus significantly inhibited the growth and proliferation of MC3T3 cells. Wong et al. reported that osteoblast growth is strongly influenced by the concentration of Mg ions in the cellular culture medium: at concentrations lower than a certain level, Mg ions can promote osteoblast proliferation, but at higher concentrations, Mg ions inhibit such growth [17].

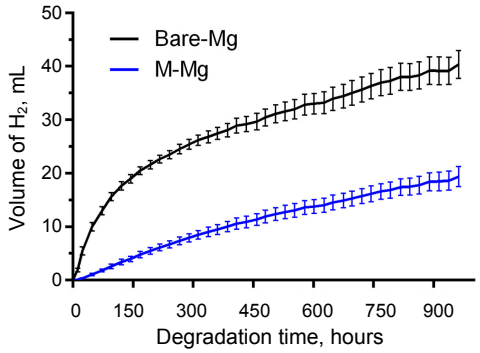

Fig. 5. Volume of hydrogen gas generated from Bare-Mg (black curve) and M-Mg (blue curve) samples immersed in SBF.

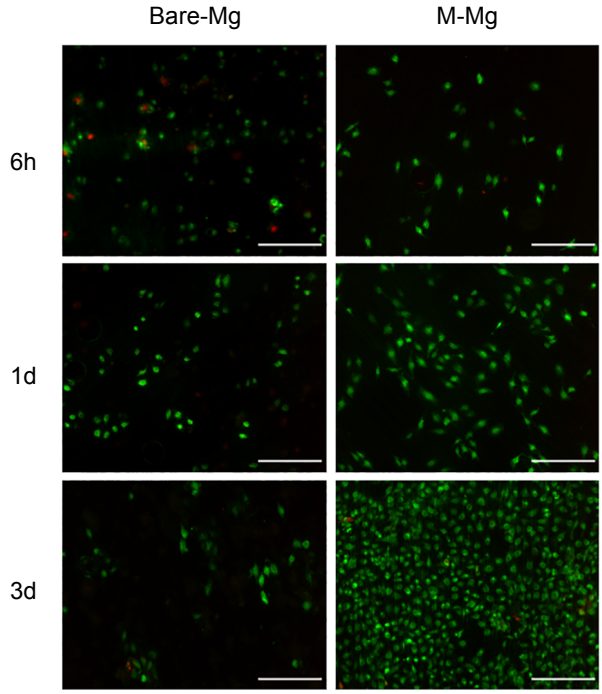

Fig. 6. Representative fluorescent microscopic images of MC3T3 cells adhered on the Bare-Mg and M-Mg surfaces after 6 h, 1 day, and 3 days. The cytoplasm of live cells was stained with calcein-AM in green, and dead cells with PI in red. Scale bar, 200 μm.

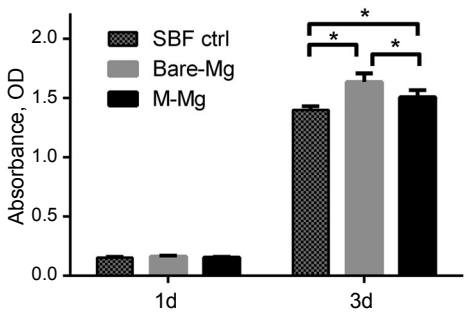

Fig. 7. Results of the CCK-8 assay for the proliferation of MC3T3 cells after incubation in the mixture of culture medium and SBF or degradation extract from Bare-Mg and M-Mg samples for 1 day or 3 days. $*p < 0.05$.

This result suggests that the reduction of Mg ion release after coating the alloy with PPC could protect osteoblasts from the growth inhibiting effects of high Mg ion concentrations and thereby promote the healing of a fractured bone.

To further understand the influence of magnesium degradation on the growth of osteoblasts, MC3T3 cells were incubated in a mixture of fresh cell culture medium with SBF or degradation extract from Bare-Mg or M-Mg collected after 26 days of degradation. According to the results of CCK-8 assays, the MC3T3 cell proliferation was similar in both culture conditions after 1 day (Fig. 7). However, after 3 days, the proliferation of cells cultured with degradation extract from Bare-Mg and M-Mg samples was significantly greater than that of cells incubated with SBF, showing good biocompatibility of the former two groups. The highest proliferation rate was observed for the cells incubated with the degradation extract from Bare-Mg. We speculate that the concentration of Mg ions in the SBF after the Mg sample degradation was relatively low due to the large ratio of the SBF volume to the Mg sample surface area as 122 mL : 1 cm^2, and therefore, the degradation extract could stimulate the proliferation of MC3T3 cells as reported by Wong et al. [17].

4. DISCUSSION

In the present study, we compared the surface morphology, roughness, hardness, wettability, degradation behaviour, and biocompatibility of Bare-Mg and M-Mg samples as potential orthopaedic implant materials. A commonly used magnesium alloy, AZ31, served as the base material to facilitate comparison with other relevant studies. We found that after coating with PPC the surface roughness of alloy samples decreased from 165.1 ± 18.8 to 136.3 ± 23.8 nm and the hardness dropped from 8.38 ± 1.21 to 0.12 ± 0.06 GPa. Meanwhile, the water contact angle of coated samples increased from 57.3 ± 3.5° to 77.6 ± 1.2°, indicating a reduction in surface wettability. More importantly, the surface PPC layer could protect AZ31 alloys from rapid degradation, which is valuable for extending the period during which the implants can provide sufficient support for fracture fixation. Furthermore, the PPC coating did not interfere with the adhesion and proliferation of osteoblasts, thus improving the biocompatibility of the implant material.

Compared to many other polymers that have been studied as coating materials for magnesium alloys, PPC offers great flexibility, which may protect implants from breakage during deformation procedures such as shaping. For example, the elongation at break of PLA and PLGA is about 5–7% [41], whereas that of PPC can reach 200–300% [42]. Furthermore, the degradation products of PPC are water and carbon dioxide, which are non-toxic and can be easily metabolized by the human body, and thus, this coating material offers good biocompatibility.

5. CONCLUSIONS

In conclusion, we successfully coated the surface of AZ31 magnesium alloys with PPC. The obtained PPC-coated AZ31 showed reductions in surface roughness, hardness, and hydrophilicity. The PPC coating layer significantly slowed the degradation of AZ31 in SBF, and cell culture experiments demonstrated a good biocompatibility of PPC-coated AZ31 for osteoblast adherence and proliferation. These results indicate that the PPC coating may extend the functional period of AZ31 magnesium implants in vivo to allow sufficient time for bone healing and stimulation of new bone formation.

ACKNOWLEDGEMENTS

The present work was supported by Talent Development Fund from the Department of Human Resources and Social Security of Jilin Province and the Development and Reform Commission of Jilin Province (2015Y038-1).

REFERENCES

1. Cauley, J. A. Osteoporosis: fracture epidemiology update 2016. *Curr. Opin. Rheumatol.*, 2017, **29**, 150–156.
2. Van Staa, T., Dennison, E., Leufkens, H., and Cooper, C. Epidemiology of fractures in England and Wales. *Bone*, 2001, **29**, 517–522.
3. Seitz, J. M., Eifler, R., Bach, F. W., and Maier, H. Magnesium degradation products: effects on tissue and

human metabolism. *J. Biomed. Mater. Res. A*, 2014, **102**, 3744–3753.
4. Niinomi, M. Recent metallic materials for biomedical applications. *Metall. Mater. Trans. A*, 2002, **33**, 477.
5. Sumner, D. Long-term implant fixation and stress-shielding in total hip replacement. *J. Biomech.*, 2015, **48**, 797–800.
6. Chen, Y., Xu, Z., Smith, C., and Sankar, J. Recent advances on the development of magnesium alloys for biodegradable implants. *Acta Biomater.*, 2014, **10**, 4561–4573.
7. Niki, Y., Matsumoto, H., Suda, Y., Otani, T., Fujikawa, K., Toyama, Y., et al. Metal ions induce bone-resorbing cytokine production through the redox pathway in synoviocytes and bone marrow macrophages. *Biomaterials*, 2003, **24**, 1447–1457.
8. Niki, Y., Matsumoto, H., Otani, T., Yatabe, T., Kondo, M., Yoshimine, F., and Toyama, Y. Screening for symptomatic metal sensitivity: a prospective study of 92 patients undergoing total knee arthroplasty. *Biomaterials*, 2005, **26**, 1019–1026.
9. Kumar, K., Gill, R., and Batra, U. Challenges and opportunities for biodegradable magnesium alloy implants. *Mater. Technol.*, 2018, **33**, 153–172.
10. Staiger, M. P., Pietak, A. M., Huadmai, J., and Dias, G. Magnesium and its alloys as orthopedic biomaterials: a review. *Biomaterials*, 2006, **27**, 1728–1734.
11. Waizy, H., Seitz, J-M., Reifenrath, J., Weizbauer, A., Bach, F-W., Meyer-Lindenberg, A., et al. Biodegradable magnesium implants for orthopedic applications. *J. Mater. Sci.*, 2013, **48**, 39–50.
12. Witte, F., Kaese, V., Haferkamp, H., Switzer, E., Meyer-Lindenberg, A., Wirth, C., and Windhagen, H. In vivo corrosion of four magnesium alloys and the associated bone response. *Biomaterials*, 2005, **26**, 3557–3563.
13. Wang, J., Tang, J., Zhang, P., Li, Y., Wang, J., Lai, Y., and Qin, L. Surface modification of magnesium alloys developed for bioabsorbable orthopedic implants: a general review. *J. Biomed. Mater. Res. B*, 2012, **100**, 1691–1701.
14. Prabhu, D. B., Gopalakrishnan, P., and Ravi, K. Coatings on implants: study on similarities and differences between the PCL coatings for Mg based lab coupons and final components. *Mater. Design*, 2017, **135**, 397–410.
15. Ostrowski, N. J., Lee, B., Roy, A., Ramanathan, M., and Kumta, P. N. Biodegradable poly(lactide-co-glycolide) coatings on magnesium alloys for orthopedic applications. *J. Mater. Sci. Mater. Med.*, 2013, **24**, 85–96.
16. Alabbasi, A., Liyanaarachchi, S., and Kannan, M. B. Polylactic acid coating on a biodegradable magnesium alloy: an in vitro degradation study by electrochemical impedance spectroscopy. *Thin Solid Films*, 2012, **520**, 6841–6844.
17. Wong, H. M., Yeung, K. W., Lam, K. O., Tam, V., Chu, P. K., Luk, K. D., and Cheung, K. M. A biodegradable polymer-based coating to control the performance of magnesium alloy orthopaedic implants. *Biomaterials*, 2010, **31**, 2084–2096.
18. Abdal-hay, A., Dewidar, M., and Lim, J. K. Biocorrosion behavior and cell viability of adhesive polymer coated magnesium based alloys for medical implants. *Appl. Surf. Sci.*, 2012, **261**, 536–546.
19. Chen, Y., Song, Y., Zhang, S., Li, J., Zhao, C., and Zhang, X. Interaction between a high purity magnesium surface and PCL and PLA coatings during dynamic degradation. *Biomed. Mater.*, 2011, **6**, 025005.
20. Kim, S. B., Jo, J. H., Lee, S. M., Kim, H. E., Shin, K. H., and Koh, Y. H. Use of a poly(ether imide) coating to improve corrosion resistance and biocompatibility of magnesium (Mg) implant for orthopedic applications. *J. Biomed. Mater. Res. A*, 2013, **101**, 1708–1715.
21. Ulery, B. D., Nair, L. S., and Laurencin, C. T. Biomedical applications of biodegradable polymers. *J. Polym. Sci. B*, 2011, **49**, 832–864.
22. Cao, H., McHugh, K., Chew, S. Y., and Anderson, J. M. The topographical effect of electrospun nanofibrous scaffolds on the in vivo and in vitro foreign body reaction. *J. Biomed. Mater. Res. A*, 2010, **93**, 1151–1159.
23. Xu, Y., Lin, L., Xiao, M., Wang, S., Smith, A. T., Sun, L., and Meng, Y. Synthesis and properties of CO_2-based plastics: environmentally-friendly, energy-saving and biomedical polymeric materials. *Prog. Polym. Sci.*, 2018, **80**, 163–182.
24. Manavitehrani, I., Fathi, A., Wang, Y., Maitz, P. K., Mirmohseni, F., Cheng, T. L., et al. Fabrication of a biodegradable implant with tunable characteristics for bone implant applications. *Biomacromolecules*, 2017, **18**, 1736–1746.
25. Xia, T., Huang, B., Ni, S., Gao, L., Wang, J., Wang, J., et al. The combination of db-cAMP and ChABC with poly(propylene carbonate) microfibers promote axonal regenerative sprouting and functional recovery after spinal cord hemisection injury. *Biomed. Pharmacother.*, 2017, **86**, 354–362.
26. Zhao, J., Han, W., Chen, H., Tu, M., Huan, S., Miao, G., et al. Fabrication and in vivo osteogenesis of biomimetic poly(propylene carbonate) scaffold with nanofibrous chitosan network in macropores for bone tissue engineering. *J. Mater. Sci. Mater. Med.*, 2012, **23**, 517–525.
27. Manavitehrani, I., Fathi, A., Wang, Y., Maitz, P. K., and Dehghani, F. Reinforced poly(propylene carbonate) composite with enhanced and tunable characteristics, an alternative for poly(lactic acid). *ACS Appl. Mater. Interfaces*, 2015, **7**, 22421–22430.
28. Oyane, A., Kim, H. M., Furuya, T., Kokubo, T., Miyazaki, T., and Nakamura, T. Preparation and assessment of revised simulated body fluids. *J. Biomed. Mater. Res. A*, 2003, **65**, 188–195.
29. Xin, Y., Hu, T., and Chu, P. In vitro studies of biomedical magnesium alloys in a simulated physiological environment: a review. *Acta Biomater.*, 2011, **7**, 1452–1459.
30. Soujanya, G. K., Hanas, T., Chakrapani, V. Y., Sunil, B. R., and Kumar, T. S. S. Electrospun nanofibrous polymer coated magnesium alloy for biodegradable implant applications. *Procedia Materials Science*, 2014, **5**, 817–823.
31. Puleo, D. and Nanci, A. Understanding and controlling the bone–implant interface. *Biomaterials*, 1999, **20**, 2311–2321.
32. Hao, L., Yang, H., Du, C., Fu, X., Zhao, N., Xu, S., et al. Directing the fate of human and mouse mesenchymal stem cells by hydroxyl–methyl mixed self-assembled

monolayers with varying wettability. *J. Mater. Chem. B*, 2014, **2**, 4794–4801.
33. Bočan, J., Maňák, J., and Jäger, A. Nanomechanical analysis of AZ31 magnesium alloy and pure magnesium correlated with crystallographic orientation. *Mater. Sci. Eng. A*, 2015, **644**, 121–128.
34. Xu, W., Yagoshi, K., Koga, Y., Sasaki, M., and Niidome, T. Optimized polymer coating for magnesium alloy-based bioresorbable scaffolds for long-lasting drug release and corrosion resistance. *Colloids Surf. B*, 2018, **163**, 100–106.
35. Jo, J-H., Li, Y., Kim, S-M., Kim, H-E., and Koh, Y-H. Hydroxyapatite/poly(ε-caprolactone) double coating on magnesium for enhanced corrosion resistance and coating flexibility. *J. Biomater. Appl.*, 2013, **28**, 617–625.
36. Zheng, Y., Gu, X., and Witte, F. Biodegradable metals. *Mater. Sci. Eng. R*, 2014, **77**, 1–34.
37. Rettig, R. and Virtanen, S. Composition of corrosion layers on a magnesium rare-earth alloy in simulated body fluids. *J. Biomed. Mater. Res. A*, 2009, **88**, 359–369.
38. Tie, D., Guan, R., Liu, H., Cipriano, A., Liu, Y., Wang, Q., et al. An in vivo study on the metabolism and osteogenic activity of bioabsorbable Mg–1Sr alloy. *Acta Biomater.*, 2016, **29**, 455–467.
39. Xu, L. and Yamamoto, A. Characteristics and cytocompatibility of biodegradable polymer film on magnesium by spin coating. *Colloids Surf. B*, 2012, **93**, 67–74.
40. Neacsu, P., Staras, A. I., Voicu, S. I., Ionascu, I., Soare, T., Uzun, S., et al. Characterization and in vitro and in vivo assessment of a novel cellulose acetate-coated Mg-based alloy for orthopedic applications. *Materials*, 2017, **10**, 686.
41. Agarwal, S., Curtin, J., Duffy, B., and Jaiswal, S. Biodegradable magnesium alloys for orthopaedic applications: a review on corrosion, biocompatibility and surface modifications. *Mater. Sci. Eng. C Mater. Biol. Appl.*, 2016, **68**, 948–963.
42. Muthuraj, R. and Mekonnen, T. Recent progress in carbon dioxide (CO2) as feedstock for sustainable materials development: co-polymers and polymer blends. *Polymer*, 2018, **145**, 348–373.

Polüpropüleenkarbonaatkatte mõju magneesiumisulami AZ31 degradatsioonile ja biosobivusele

Zhiwei Zhao, Lirong Zhao, Xudong Shi, Jianfeng Liu, Yijun Wang, Wu Xu, Hai Sun, Zhuo Fu, Bin Liu ja Shucheng Hua

Magneesiumisulamite kasutust degradeeruvates ortopeedilistes implantaatides limiteerib nende liiga kiire lagunemine organismis ja sellest tulenev mehaanilise tugevuse vähenemine enne luu piisavat taastumist. Selle puuduse kõrvaldamise eesmärgil katsime magneesiumisulami AZ31 pinna polüpropüleenkarbonaat- (PPC) kattega. Saadud PPC-kattega AZ31-l on katteta materjaliga võrreldes väiksem pinnakaredus, tugevus ja hüdrofiilsus. PPC-kattega sulami AZ31 degradatsioonikiirus kunstlikus kehavedelikus osutus samuti tunduvalt väiksemaks. Osteoblastsete rakkude kultuuri MC3T3 adherentsus ja kiire kasv näitasid PPC-kattega AZ31 head biosobivust. Käesoleva uurimuse tulemused näitavad, et PPC-katte kasutamine võib pikendada magneesiumisulami AZ31 funktsionaalset perioodi organismis, andes luu taastumiseks piisavalt aega ja stimuleerides uue luukoe teket.